International Journal of Nanomedicine

Dovepress
open access to scientific and medical research

Open Access Full Text Article

ORIGINAL RESEARCH

In vitro cytotoxicity of SiO_2 or ZnO nanoparticles with different sizes and surface charges on U373MG human glioblastoma cells

This article was published in the following Dove Press journal:
International Journal of Nanomedicine
15 December 2014
Number of times this article has been viewed

Jung-Eun Kim[1,*]
Hyejin Kim[1,*]
Seong Soo A An[2]
Eun Ho Maeng[3]
Meyoung-Kon Kim[4]
Yoon-Jae Song[1]

[1]Department of Life Science, [2]Department of Bionano Technology, Gachon University, Seongnam-Si, South Korea; [3]Korea Testing and Research Institute, Seoul, South Korea; [4]Department of Biochemistry and Molecular Biology, Korea University Medical School and College, Seoul, South Korea

*These authors contributed equally to this work

Abstract: Silicon dioxide (SiO_2) and zinc oxide (ZnO) nanoparticles are widely used in various applications, raising issues regarding the possible adverse effects of these metal oxide nanoparticles on human cells. In this study, we determined the cytotoxic effects of differently charged SiO_2 and ZnO nanoparticles, with mean sizes of either 100 or 20 nm, on the U373MG human glioblastoma cell line. The overall cytotoxicity of ZnO nanoparticles against U373MG cells was significantly higher than that of SiO_2 nanoparticles. Neither the size nor the surface charge of the ZnO nanoparticles affected their cytotoxicity against U373MG cells. The 20 nm SiO_2 nanoparticles were more toxic than the 100 nm nanoparticles against U373MG cells, but the surface charge had little or no effect on their cytotoxicity. Both SiO_2 and ZnO nanoparticles activated caspase-3 and induced DNA fragmentation in U373MG cells, suggesting the induction of apoptosis. Thus, SiO_2 and ZnO nanoparticles appear to exert cytotoxic effects against U373MG cells, possibly via apoptosis.

Keyword: apoptosis

Introduction

Nanoparticles (NPs) are objects with at least one dimension less than 100 nm.[1] Many NPs offer unique and beneficial properties, and they have been widely used in medical, pharmaceutical, food, cosmetics, electronics, and other industries (reviewed in Uskokovic).[2] Silicon dioxide (SiO_2) and zinc oxide (ZnO) NPs have photocatalytic activities and are commonly used in various consumer products (eg, cosmetics) and biomedical applications (eg, drug delivery and theranostics) (reviewed in Fan and Lu[3] and Fine et al[4]).

Given their widespread use, humans are constantly exposed to SiO_2 and ZnO NPs, which can enter the body via ingestion, inhalation, and dermal absorption.[5] NPs may interact with tissue macromolecules and adversely affect cellular physiology.[6–10] Numerous studies have investigated the cytotoxic effects of SiO_2 and ZnO NPs,[11–19] but many controversies remain due to the physical and chemical properties of these NPs.

Furthermore, we do not yet fully understand the underlying cell-death mechanisms induced by SiO_2 and ZnO NPs. For example, SiO_2 and ZnO NPs reportedly trigger the intrinsic apoptotic pathway by generating reactive oxygen species (ROS) and inducing the p53 pathway to activate the caspase cascade.[20–23] Both SiO_2 and ZnO NPs were shown to activate the initiator caspase-9 and the executioner caspase-3 in human lung epithelial cells and dermal fibroblasts.[20–23] However, a recent study found that ZnO NP-mediated apoptosis was not related to ROS generation or the p53 pathway.[24] Thus, the

Correspondence: Yoon-Jae Song
Department of Life Science,
Gachon University, San 65,
Bokjeong-Dong, Sujeong-Gu,
Seongnam-Si 461-701, South Korea
Tel +82 31 750 8731
Fax +82 31 750 8573
Email songyj@gachon.ac.kr

Correspondence: Meyoung-Kon Kim
Department of Biochemistry and
Molecular Biology, Korea University
Medical School and College,
Anam-Dong 5 Ga, Seoungbuk-Gu,
Seoul 135-701, South Korea
Tel +82 2 920 6184
Fax +82 2 923 0480
Email jerry@korea.ac.kr

cell-death pathways mediated by SiO_2 and ZnO NPs are still the subject of some debate.

In this study, we investigated the cytotoxic effects of SiO_2 and ZnO NPs on the U373MG human glioblastoma cell line. Since cytotoxic potentials may be affected by the physical and chemical properties of NPs, such as their sizes and surface charges, we selected SiO_2 and ZnO NPs of different sizes (100 nm and 20 nm) and surface charges and examined their cytotoxic and apoptotic effects on U373MG cells.

Materials and methods

Cells, reagents, and preparation of NPs

The U373MG cells were maintained in Dulbecco's Modified Eagle's Medium (Biowest, Nuaille, France) supplemented with 10% fetal bovine serum (Biowest), penicillin (100 U/mL), and streptomycin (100 µg/mL). Zinc chloride was purchased from Sigma-Aldrich (St Louis, MO, USA). The 20 and 100 nm ZnO NPs were purchased from Sumitomo Osaka Cement Co, Ltd (Lot number 141319) (Tokyo, Japan) and American Elements (Lot number 1871511079-673) (Los Angeles, CA, USA), respectively. The surface charge of the ZnO NPs was modified with citrate (for a negative charge) and L-serine (for a positive charge), as previously reported.[25] The 20 and 100 nm SiO_2 NPs were purchased from E&B Nanotech Co, Ltd (Ansan-si, South Korea). To reduce their negative charge, the SiO_2 NPs were treated with L-arginine (R). Detailed information regarding the characterizations and physicochemical properties of the SiO_2 and ZnO NPs can be found in Kim et al.[26]

Western blot analysis

Cell lysates were harvested, fractionated, and transferred to nitrocellulose membranes as described previously.[27] Antibodies to poly-(adenosine diphosphate [ADP]-ribose) polymerase (PARP) and alpha-tubulin were purchased from Cell Signaling Technology (Beverly, MA, USA) and Sigma-Aldrich, respectively. Enhanced chemiluminescence detection reagents (Thermo Fisher Scientific, Waltham, MA, USA) and secondary peroxidase-labeled anti-mouse or anti-rabbit immunoglobulin G antibodies (Amersham Biosciences, Piscataway, NJ, USA) were used according to the manufacturer's directions.

Cell viability and DNA fragmentation assays

Cell viability was determined by using the CellTiter-Glo luminescent cell viability assay (Promega Corporation, Madison, WI, USA) according to the manufacturer's directions. DNA fragmentation was determined by using the DeadEnd™ Fluorometric terminal deoxynucleotidyl transferase-mediated dUTP nick end labeling (TUNEL) System (Promega Corporation) according to the manufacturer's directions. Nuclei were stained using Vectasheild mounting medium with DAPI (Vector Laboratories, Inc., Burlingame, CA, USA).

Results

Effect of SiO_2 or ZnO NPs on the viability of U373MG human glioblastoma cells

The U373MG cells were treated with various concentrations of SiO_2 or ZnO NPs with different sizes and surface charges ($ZnO^{AE100(+)}$, $ZnO^{AE100(-)}$, $ZnO^{SM20(+)}$, $ZnO^{SM20(-)}$, $SiO_2^{EN100(R)}$, $SiO_2^{EN100(-)}$, $SiO_2^{EN20(R)}$, and $SiO_2^{EN20(-)}$). After 24 hours, cell viability was measured using the CellTiter-Glo assay, which determines the presence of live and metabolically active cells by measuring adenosine triphosphate (Figure 1). Treatment with 6 mg/mL of $SiO_2^{EN100(R)}$ and $SiO_2^{EN100(-)}$ reduced the viability of U373MG cells by 68% and 65%, respectively (Figure 1A and B). Interestingly, the 20 nm SiO_2 NPs were more toxic to U373MG cells than 100 nm SiO_2 NPs. Treatment with 0.6 and 0.9 mg/mL of $SiO_2^{EN20(R)}$ reduced the viability of U373MG cells by 90% and 98%, respectively (Figure 1C). Similarly, treatment with 0.6 and 0.8 mg/mL of $SiO_2^{EN20(-)}$ reduced the viability of U373MG cells by 23% and 96%, respectively (Figure 1D). The cytotoxicity of SiO_2 NPs was not cell-type specific as we observed similar levels of cytotoxicity against human dermal fibroblast and HCT116 human colorectal carcinoma cells (data not shown). The half-maximal inhibitory concentration values for the cytotoxicity of $SiO_2^{EN100(R)}$, $SiO_2^{EN100(-)}$, $SiO_2^{EN20(R)}$, and $SiO_2^{EN20(-)}$ against U373MG cells at 24 hours after treatment were 4.36, 4.93, 0.41, and 0.68 mg/mL, respectively (Table 1).

Compared to the SiO_2 NPs, the ZnO NPs were significantly more toxic to U373MG cells as treatment with 20 µg/mL of $ZnO^{AE100(+)}$, $ZnO^{AE100(-)}$, $ZnO^{SM20(+)}$, and $ZnO^{SM20(-)}$ for 24 hours reduced the viability of U373MG cells by 53%, 47%, 74%, and 53%, respectively (Figure 2). The half-maximal inhibitory concentration values for the cytotoxicity of $ZnO^{AE100(+)}$, $ZnO^{AE100(-)}$, $ZnO^{SM20(+)}$, and $ZnO^{SM20(-)}$ on U373MG cells at 24 hours after treatment were 19.67, 20.47, 16.82, and 19.67 µg/mL, respectively (Table 1). Since treatment with 20 µg/mL of zinc chloride exhibited no cytotoxic effect against U373MG cells, the observed cytotoxicity appeared to have been due to the effect of the ZnO NPs (rather than Zn_2^+) on U373MG cells (Figure 3).

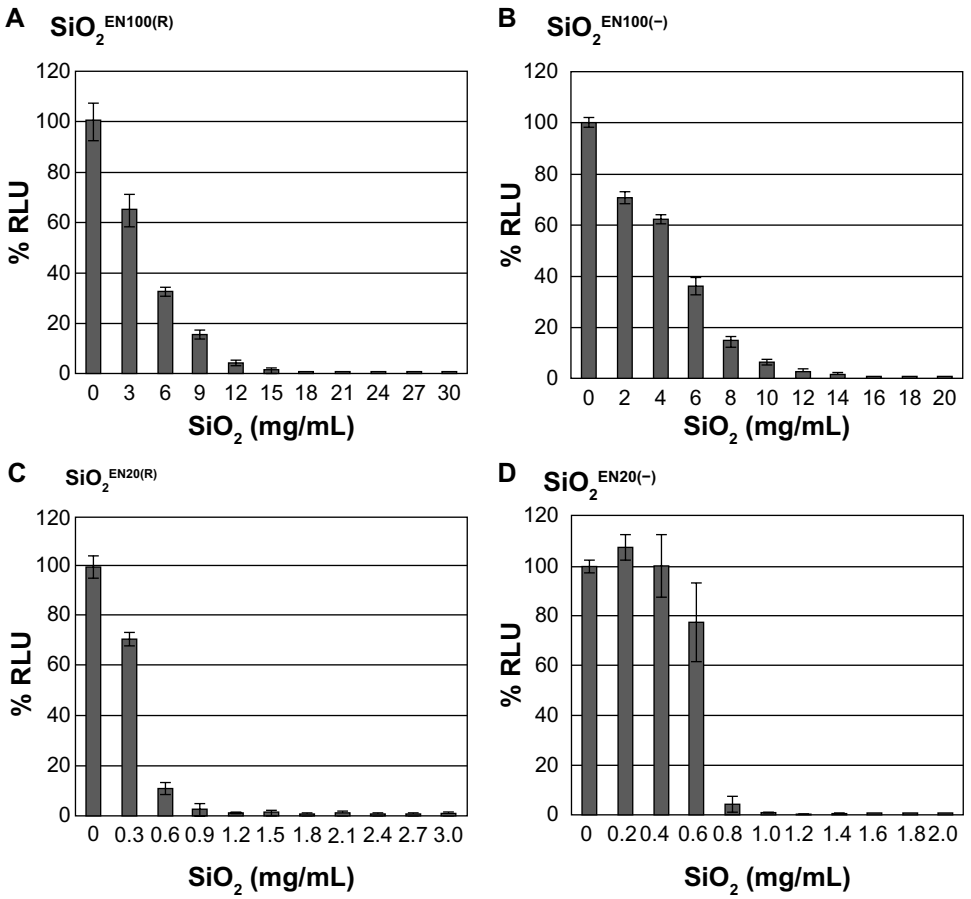

Figure 1 The effect of SiO_2 NPs on the viability of U373MG cells.
Notes: U373MG cells were treated with various concentration of (**A**) $SiO_2^{EN100(R)}$, (**B**) $SiO_2^{EN100(-)}$, (**C**) $SiO_2^{EN20(R)}$, or (**D**) $SiO_2^{EN20(-)}$ NPs. At 24 hours after treatment, cell viability was determined with the CellTiter-Glo assay. To calculate the relative luciferase activities, the luciferase activities at 0 hours after treatment were set to 100%. The data shown here represent the results from three independent experiments.
Abbreviations: NPs, nanoparticles; RLU, relative luminescence units; SiO_2, silicon dioxide.

Taken together, these results indicate that the ZnO NPs were more toxic than SiO_2 NPs against U373MG cells. Furthermore, the 20 nm SiO_2 NPs were more toxic than the 100 nm NPs, whereas the cytotoxicity of ZnO NPs was not affected by their size or surface charge in our experimental systems.

Table 1 The IC_{50} values for the cytotoxicity of SiO_2 or ZnO NPs against U373MG cells at 24 hours

NPs	IC_{50} (μg/mL)
$ZnO^{AE100(+)}$	19.67±0.78
$ZnO^{AE100(-)}$	20.47±0.84
$ZnO^{SM20(+)}$	16.82±0.42
$ZnO^{SM20(-)}$	19.67±1.85
$SiO_2^{EN100(R)}$	4,360.0±0.10
$SiO_2^{EN100(-)}$	4,930.0±0.16
$SiO_2^{EN20(R)}$	410.0±0.01
$SiO_2^{EN20(-)}$	680.0±0.03

Abbreviations: IC_{50}, half-maximal inhibitory concentration; NPs, nanoparticles; SiO_2, silicon dioxide; ZnO, zinc oxide.

Effect of SiO_2 or ZnO NPs on caspase-3 activation

To determine whether SiO_2 or ZnO NPs induce apoptosis, U373MG cells were treated with the above-described SiO_2 or ZnO NPs, and caspase-3 activation was assessed by determining the proteolytic cleavage of PARP (from the native 116 kDa to 89 kDa) at 0, 1, 3, 6, and 9 hours after treatment. The treatment of U373MG cells with SiO_2 NPs at the concentrations shown to reduce cell viability by 85% to 90% was found to rapidly induce PARP cleavage at 1 hour after treatment (Figure 4; compare lane 2 with lane 1). $ZnO^{AE100(-)}$ and $ZnO^{SM20(-)}$ also rapidly induced PARP cleavage in U373MG cells at 1 hour after treatment (Figure 5A and B; compare lane 2 with lane 1), whereas $ZnO^{AE100(+)}$ and $ZnO^{SM20(+)}$ induced PARP cleavage at later time points at 9 and 6 hour, respectively (Figure 5C and D; compare lane 2 with lane 1). These data indicate that both SiO_2 and ZnO NPs induce caspase-3 activation, further suggesting that they both induce apoptosis.

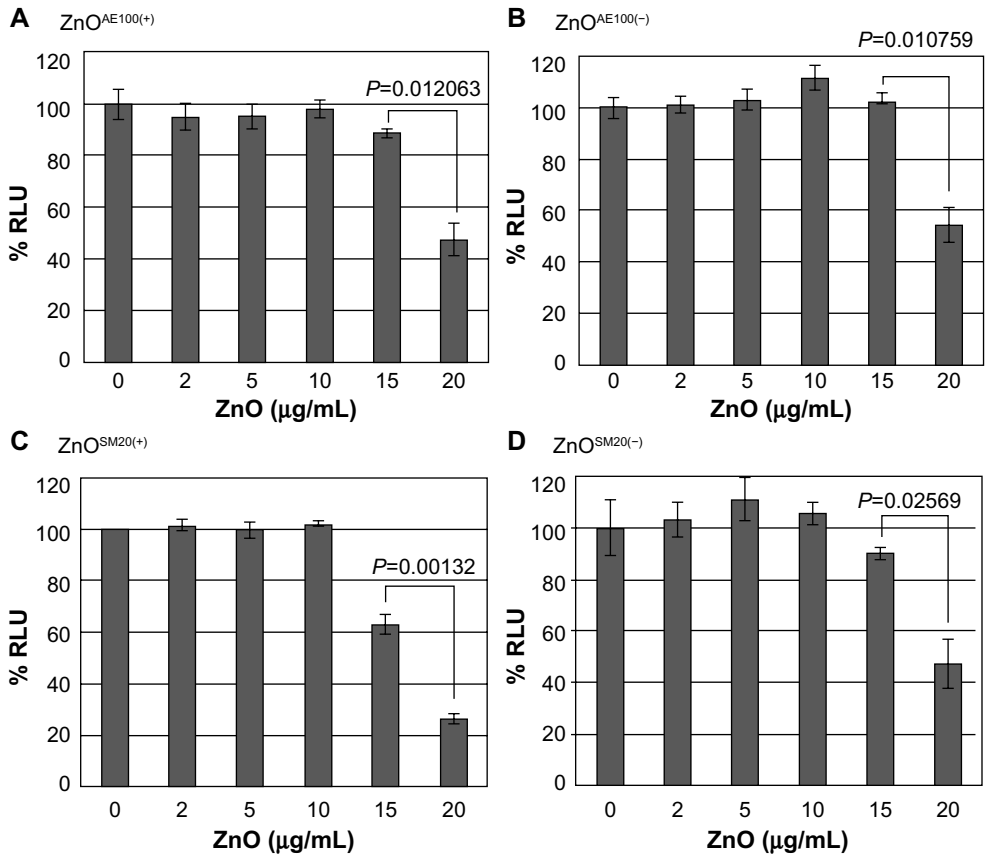

Figure 2 The effect of ZnO NPs on the viability of U373MG cells.
Notes: U373MG cells were treated with 0, 2, 5, 10, 15, or 20 μg/mL of (**A**) $ZnO^{AE100(+)}$, (**B**) $ZnO^{AE100(-)}$, (**C**) $ZnO^{SM20(+)}$, or (**D**) $ZnO^{SM20(-)}$ NPs. At 24 hours after treatment, cell viability was determined with the CellTiter-Glo assay. To calculate the relative luciferase activities, the luciferase activities at 0 hours after treatment were set to 100%. The data shown here represent the results from three independent experiments. Significant differences between samples were determined by the *P*-value of a two-sample *t*-test ($P<0.05$).
Abbreviations: NPs, nanoparticles; RLU, relative luminescence units; ZnO, zinc oxide.

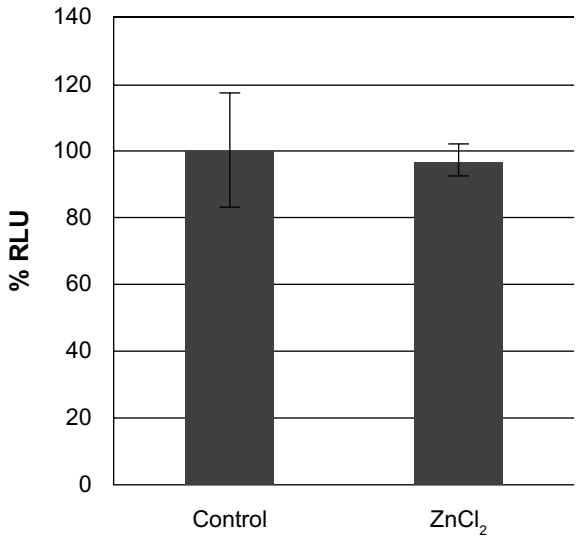

Figure 3 The effect of non-nano $ZnCl_2$ on the viability of U373MG cells.
Notes: U373MG cells were treated with or without 20 μg/mL $ZnCl_2$. At 24 hours after treatment, cell viability was determined with the Celltiter-Glo assay. To calculate the relative luciferase activities, the luciferase activities of mock-treated cells were set to 100%. The data shown here represent the results from three independent experiments.
Abbreviations: RLU, relative light unit; $ZnCl_2$, zinc chloride.

Effect of SiO_2 or ZnO NPs on chromosomal DNA fragmentation and damage

To further assess the apoptotic effects of SiO_2 or ZnO NPs, U373MG cells were treated with the above-described NPs

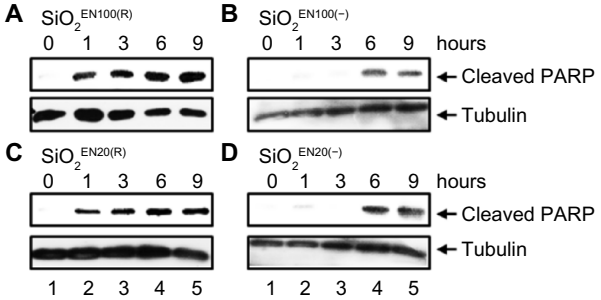

Figure 4 The effect of SiO_2 NPs on caspase activation.
Notes: U373MG cells were treated with 9 mg/mL of (**A**) $SiO_2^{EN100(R)}$ or (**B**) $SiO_2^{EN100(-)}$ NPs, or 0.8 mg/mL of (**C**) $SiO_2^{EN20(R)}$ or (**D**) $SiO_2^{EN20(-)}$ NPs. At 0, 1, 3, 6 and 9 hours after treatment, PARP cleavage was determined by Western blot analysis.
Abbreviations: NPs, nanoparticles; PARP, poly-(adenosine diphosphate-ribose) polymerase; SiO_2, silicon dioxide.

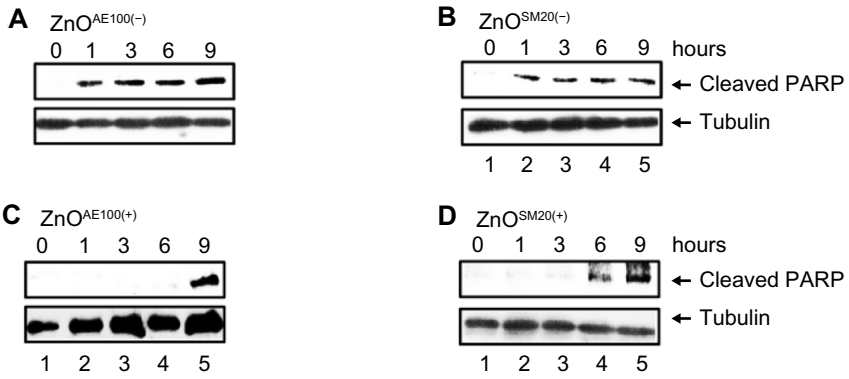

Figure 5 The effect of ZnO nanoparticles on caspase activation.
Notes: U373MG cells were treated with 20 μg/mL of (**A**) $ZnO^{AE100(-)}$, (**B**) $ZnO^{SM20(-)}$, (**C**) $ZnO^{AE100(+)}$, or (**D**) $ZnO^{SM20(+)}$ NPs. At 0, 1, 3, 6, 9 hours after treatment, PARP cleavage was determined by Western blot analysis.
Abbreviations: NPs, nanoparticles; PARP, poly-(adenosine diphosphate-ribose) polymerase; ZnO, zinc oxide.

for 6 hours, and chromosomal DNA fragmentation was determined using a TUNEL assay. As expected, SiO_2 NPs and ZnO NPs induced chromosomal DNA fragmentation in U373MG cells (Figure 6). At 6 hours after treatment with $SiO_2^{EN100(R)}$, $SiO_2^{EN100(-)}$, $SiO_2^{EN20(R)}$, and $SiO_2^{EN20(-)}$, 11.7%, 12.9%, 10.8%, and 10.1% of the cells were found to be TUNEL positive (Figure 6A). Compared to the SiO_2 NPs, the ZnO NPs were more potent in inducing chromosomal DNA fragmentation as 42.7%, 60.4%, 42.8%, and 19.5% of the cells treated with $ZnO^{AE100(+)}$, $ZnO^{AE100(-)}$, $ZnO^{SM20(+)}$, and $ZnO^{SM20(-)}$, respectively, were found to be TUNEL positive (Figure 6B). These data suggest that the ZnO NPs may be more effective at inducing chromosomal DNA fragmentation in these cells (Figure 6B). In addition to the TUNEL assay, the comet assay was employed to examine DNA damage in SiO_2 or ZnO NP-treated cells. Consistent with the TUNEL data, both SiO_2 and ZnO NPs induced DNA damage in U373MG cells (data not shown). Taken together, these data indicate that both SiO_2 and ZnO NPs reduce the viability of U373MG cells by inducing apoptosis, and further suggest that ZnO NPs may be more effective than SiO_2 NPs for inducing apoptosis in U373MG cells.

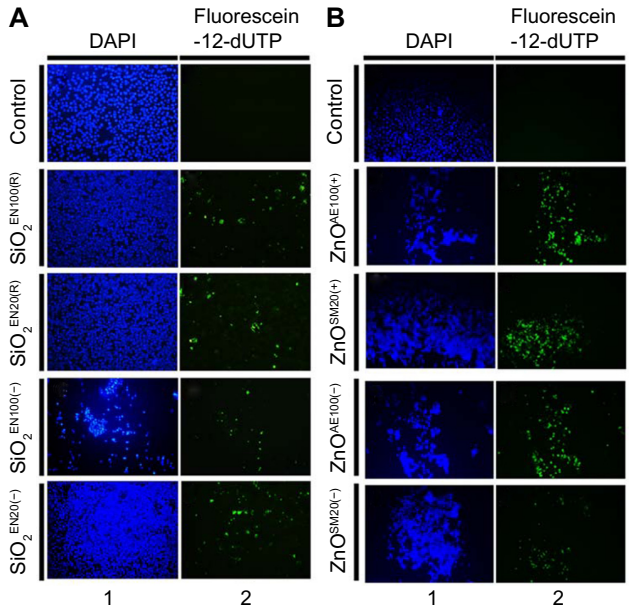

Figure 6 The effect of SiO_2 or ZnO NPs on DNA fragmentation.
Notes: U373MG cells were treated with (**A**) SiO_2 or (**B**) ZnO NPs with different sizes and surface charges at the concentrations described above. At 6 hours after treatment, fragmented DNA was labeled with fluorescein-12-UTP (green) and visualized under fluorescence microscopy. Nuclei were visualized by DAPI staining (blue).
Abbreviations: DAPI, 4′,6-diamidino-2-phenylindole; NPs, nanoparticles; SiO_2, silicon dioxide; ZnO, zinc oxide; UTP, uridine triphosphate.

Discussion

In the present study, we investigated the cytotoxic effects of SiO_2 and ZnO NPs with two different sizes (20 and 100 nm) and charges (positive and negative) against the U373MG human glioblastoma cell line. The SiO_2 and ZnO NPs both reduced the viability of U373MG cells at 24 hours after treatment. The $ZnO^{SM20(+)}$, $ZnO^{SM20(-)}$, $ZnO^{AE100(+)}$, and $ZnO^{AE100(-)}$ NPs were 24-, 34-, 222-, and 241-fold more toxic to U373MG cells than their corresponding SiO_2 NP counterparts. These differences in the cytotoxicities of the SiO_2 and ZnO NPs may reflect differences in solubility, dissolution rate in the media, protein interactions, ROS generation, and/or the ability to activate the intrinsic apoptotic and/or necrotic pathways.

Other studies have indicated that both size and surface charge can influence the cytotoxicity of SiO_2 and ZnO NPs.[28–31] Consistent with these studies, we observed that particle size affected the cytotoxicity of $SiO_2^{EN20(R)}$ and $SiO_2^{EN20(-)}$ NPs, which were, respectively, eleven- and seven-fold more toxic than 100 nm counterparts against U373MG

cells. Smaller NPs may be more effective at entering cells and organelles (eg, mitochondria), allowing them more opportunity to induce oxidative stress and apoptosis.[14,31–33] In contrast to the previous reports, however, we found that the surface charge of SiO_2 NPs had almost no effect on their cytotoxicity against U373MG cells. Although $SiO_2^{EN100(R)}$ and $SiO_2^{EN20(R)}$ NPs were slightly more toxic than $SiO_2^{EN100(-)}$ and $SiO_2^{EN20(-)}$, respectively, these differences were not significant. Also, inconsistent with the previous reports, we found that the cytotoxicity of ZnO NPs against U373MG cells was unaffected by their size and surface charge. Future work will be needed to examine these apparent discrepancies.

Treatment of U373MG cells with SiO_2 NPs was found to rapidly activate caspase-3 and induce apoptosis within 1 hour. Treatment with $ZnO^{AE100(-)}$ and $ZnO^{SM20(-)}$ NPs also activated caspase-3 by 1 hour after treatment, whereas $ZnO^{AE100(+)}$ and $ZnO^{SM20(+)}$ activated caspase-3 later (9 and 6 hours after treatment, respectively). Previous reports showed that SiO_2 and ZnO NPs may induce the intrinsic pathway for apoptosis via ROS-mediated p53 activation.[20–23] ROS-induced DNA damage activates p53, which triggers apoptosis by transactivating proapoptotic genes and activating other transcription-independent mechanisms.[34] However, Wilhelmi et al reported that ZnO NPs induce necrosis and apoptosis in macrophages via ROS- and p53-independent pathway.[24] Consistent with the latter study, we found that both SiO_2 and ZnO NPs induced apoptosis in U373MG cells, which express mutant p53. Other authors have suggested that, in addition to the ROS-mediated p53 activation pathway, SiO_2 and ZnO NPs may activate the p38 mitogen-activated protein kinase and/or c-Jun N-terminal kinase pathways to transactivate proapoptotic genes and induce apoptosis.[23,35]

Since DNA damage induces the G_2/M DNA damage checkpoint to arrest the cell cycle,[36] it is not surprising that silica NPs induce cell cycle arrest at the G_2/M phase.[37] More specifically, they induce the G_2/M DNA damage checkpoint via the activation of Chk1, which phosphorylates p53.[37,38] Since Cdk2 has been reported to play an important role in p53-independent G_2/M checkpoint control,[39] we speculate that SiO_2 and ZnO NPs may arrest the cell cycle at the G_2/M phase in U373MG cells, possibly via a Cdk2-dependent pathway. In addition to apoptosis, SiO_2 and ZnO NPs may induce necrotic cell death in U373MG cells. Thus, further studies are needed to examine how SiO_2 and ZnO NPs induce apoptotic and/or necrotic cell death in human cell lines.

Conclusion

We herein investigated the cytotoxic effects of SiO_2 and ZnO NPs with different sizes and surface charges on the human glioblastoma cell line, U373MG. The overall cytotoxicity of the ZnO NPs was significantly higher than that of the SiO_2 NPs against U373MG cells. The cytotoxicity of the SiO_2 NPs was affected by the particle size, but not the surface charge, in our system, with the smaller SiO_2 NPs showing a higher cytotoxicity. In contrast, changes in the size and surface charge of the ZnO NPs had little or no effect on their cytotoxicity against U373MG cells. Both SiO_2 and ZnO NPs were found to activate caspase-3 and induce DNA fragmentation in our system. Thus, we report that the tested SiO_2 and ZnO NPs exhibited cytotoxic effects against U373MG cells, at least partly via the induction of apoptosis.

Acknowledgment

This research was supported by a grant (10182MFDS991) from the Ministry of Food and Drug Safety in 2010–2011.

Disclosure

The authors report no conflict of interest in this work.

References

1. Ma H, Williams PL, Diamond SA. Ecotoxicity of manufactured ZnO nanoparticles – a review. *Environ Pollut*. 2013;172:76–85.
2. Uskoković V. Entering the era of nanoscience: time to be so small. *J Biomed Nanotechnol*. 2013;9(9):1441–1470.
3. Fan Z, Lu JG. Zinc oxide nanostructures: synthesis and properties. *J Nanosci Nanotechnol*. 2005;5(10):1561–1573.
4. Fine D, Grattoni A, Goodall R, et al. Silicon micro- and nanofabrication for medicine. *Adv Healthc Mater*. 2013;2(5):632–666.
5. Nasir A. Nanotechnology and dermatology: part II – risks of nanotechnology. *Clin Dermatol*. 2010;28(5):581–588.
6. Deng ZJ, Mortimer G, Schiller T, Musumeci A, Martin D, Minchin RF. Differential plasma protein binding to metal oxide nanoparticles. *Nanotechnology*. 2009;20(45):455101.
7. Lundqvist M, Stigler J, Cedervall T, et al. The evolution of the protein corona around nanoparticles: a test study. *ACS Nano*. 2011;5(9):7503–7509.
8. Okoturo-Evans O, Dybowska A, Valsami-Jones E, et al. Elucidation of toxicity pathways in lung epithelial cells induced by silicon dioxide nanoparticles. *PLoS One*. 2013;8(9):e72363.
9. Ekkapongpisit M, Giovia A, Follo C, Caputo G, Isidoro C. Biocompatibility, endocytosis, and intracellular trafficking of mesoporous silica and polystyrene nanoparticles in ovarian cancer cells: effects of size and surface charge groups. *Int J Nanomedicine*. 2012;7:4147–4158.
10. Lee SH, Pie JE, Kim YR, Lee HR, Son SW, Kim MK. Effects of zinc oxide nanoparticles on gene expression profile in human keratinocytes. *Mol Cell Toxicol*. 2012;8(2):113–118.
11. Bauer AT, Strozyk EA, Gorzelanny C, et al. Cytotoxicity of silica nanoparticles through exocytosis of von Willebrand factor and necrotic cell death in primary human endothelial cells. *Biomaterials*. 2011;32(33):8385–8393.

12. Rabolli V, Thomassen LC, Princen C, et al. Influence of size, surface area and microporosity on the in vitro cytotoxic activity of amorphous silica nanoparticles in different cell types. *Nanotoxicology*. 2010;4(3):307–318.
13. Corbalan JJ, Medina C, Jacoby A, Malinski T, Radomski MW. Amorphous silica nanoparticles trigger nitric oxide/peroxynitrite imbalance in human endothelial cells: inflammatory and cytotoxic effects. *Int J Nanomedicine*. 2011;6:2821–2835.
14. Xia T, Kovochich M, Liong M, et al. Comparison of the mechanism of toxicity of zinc oxide and cerium oxide nanoparticles based on dissolution and oxidative stress properties. *ACS Nano*. 2008;2(10):2121–2134.
15. Sharma V, Anderson D, Dhawan A. Zinc oxide nanoparticles induce oxidative stress and genotoxicity in human liver cells (HepG2). *J Biomed Nanotechnol*. 2011;7(1):98–99.
16. Sharma V, Singh P, Pandey AK, Dhawan A. Induction of oxidative stress, DNA damage and apoptosis in mouse liver after sub-acute oral exposure to zinc oxide nanoparticles. *Mutat Res*. 2012;745(1–2):84–91.
17. Sharma V, Anderson D, Dhawan A. Zinc oxide nanoparticles induce oxidative DNA damage and ROS-triggered mitochondria mediated apoptosis in human liver cells (HepG2). *Apoptosis*. 2012;17(8):852–870.
18. Cho WS, Duffin R, Poland CA, et al. Metal oxide nanoparticles induce unique inflammatory footprints in the lung: important implications for nanoparticle testing. *Environ Health Perspect*. 2010;118(12):1699–1706.
19. Kermanizadeh A, Pojana G, Gaiser BK, et al. In vitro assessment of engineered nanomaterials using a hepatocyte cell line: cytotoxicity, pro-inflammatory cytokines and functional markers. *Nanotoxicology*. 2013;7(3):301–313.
20. Xu Z, Chou L, Sun J. Effects of SiO_2 nanoparticles on HFL-I activating ROS-mediated apoptosis via p53 pathway. *J Appl Toxicol*. 2012;32(5):358–364.
21. Ahamed M. Silica nanoparticles-induced cytotoxicity, oxidative stress and apoptosis in cultured A431 and A549 cells. *Hum Exp Toxicol*. 2013;32(2):186–195.
22. Ahamed M, Akhtar MJ, Raja M, et al. ZnO nanorod-induced apoptosis in human alveolar adenocarcinoma cells via p53, survivin and bax/bcl-2 pathways: role of oxidative stress. *Nanomedicine*. 2011;7(6):904–913.
23. Meyer K, Rajanahalli P, Ahamed M, Rowe JJ, Hong Y. ZnO nanoparticles induce apoptosis in human dermal fibroblasts via p53 and p38 pathways. *Toxicol In Vitro*. 2011;25(8):1721–1726.
24. Wilhelmi V, Fischer U, Weighardt H, et al. Zinc oxide nanoparticles induce necrosis and apoptosis in macrophages in a p47phox- and Nrf2-independent manner. *PLoS One*. 2013;8(6):e65704.
25. Kim K-M, Kim T-H, Kim H-M, et al. Colloidal behaviors of ZnO nanoparticles in various aqueous media. *Toxicol Environ Health Sci*. 2012;4(2):121–131.
26. Kim KM, Choi MH, Lee JK, et al. Physicochemical properties of surface charge-modified ZnO nanomaterials with different particle sizes. In press 2014.
27. Song YJ, Stinski MF. Inhibition of cell division by the human cytomegalovirus IE86 protein: role of the p53 pathway or cyclin-dependent kinase 1/cyclin B1. *J Virol*. 2005;79(4):2597–2603.
28. Park YH, Bae HC, Jang Y, et al. Effect of the size and surface charge of silica nanoparticles on cutaneous toxicity. *Mol Cell Toxicol*. 2013;9(1):67–74.
29. Greish K, Thiagarajan G, Herd H, et al. Size and surface charge significantly influence the toxicity of silica and dendritic nanoparticles. *Nanotoxicology*. 2012;6(7):713–723.
30. Pujalté I, Passagne I, Brouillaud B, et al. Cytotoxicity and oxidative stress induced by different metallic nanoparticles on human kidney cells. *Part Fibre Toxicol*. 2011;8:10.
31. Malvindi MA, Brunetti V, Vecchio G, Galeone A, Cingolani R, Pompa PP. SiO_2 nanoparticles biocompatibility and their potential for gene delivery and silencing. *Nanoscale*. 2012;4(2):486–495.
32. Bae HC, Ryu HJ, Jeong SH, et al. Oxidative stress and apoptosis induced by ZnO nanoparticles in HaCaT cells. *Mol Cell Toxicol*. 2011;7(4):333–337.
33. Hsiao IL, Huang YJ. Effects of various physicochemical characteristics on the toxicities of ZnO and TiO nanoparticles toward human lung epithelial cells. *Sci Total Environ*. 2011;409(7):1219–1228.
34. Speidel D. Transcription-independent p53 apoptosis: an alternative route to death. *Trends Cell Biol*. 2010;20(1):14–24.
35. McNamee LM, Brodsky MH. p53-independent apoptosis limits DNA damage-induced aneuploidy. *Genetics*. 2009;182(2):423–435.
36. Cuddihy AR, O'Connell MJ. Cell-cycle responses to DNA damage in G2. *Int Rev Cytol*. 2003;222:99–140.
37. Duan J, Yu Y, Li Y, Zhou X, Huang P, Sun Z. Toxic effect of silica nanoparticles on endothelial cells through DNA damage response via Chk1-dependent G2/M checkpoint. *PLoS One*. 2013;8(4):e62087.
38. Ou YH, Chung PH, Sun TP, Shieh SY. p53 C-terminal phosphorylation by CHK1 and CHK2 participates in the regulation of DNA-damage-induced C-terminal acetylation. *Mol Biol Cell*. 2005;16(4):1684–1695.
39. Chung JH, Bunz F. Cdk2 is required for p53-independent G2/M checkpoint control. *PLoS Genet*. 2010;6(2):e1000863.